ECE 445

SENIOR DESIGN LABORATORY

FINAL REPORT

Final Report for ECE445 Autonomous Transport Car

Team #43

YIQI TAO (yiqitao2)
XUBIN SHEN (xubins3)
JINGYUAN MA (jm53)
HAOTIAN ZHANG (hz75)

Sponsor: Chushan Li

May 8, 2025

Abstract

The demand for efficient express package handling has surged due to the development of e-commerce, placing a significant pressure on manual picking at warehouses. These systems often suffer from low efficiency, high labor costs, and increased error rates—particularly during peak periods. To address this challenge, we propose an intelligent autonomous transport system equipped with real-time navigation, obstacle avoidance, and a smart robotic arm based on color label recognition. By integrating automation with human oversight, the proposed system enhances operational efficiency, reduces labor dependency, and significantly improves the user experience in express logistics environments.

Contents

1 Introduction

1.1 Problem and Solution

With the rapid development of e-commerce, online shopping has become an integral part of daily life. This surge in consumer activity has led to an exponential increase in express delivery volumes. However, the existing storage and retrieval systems for express packages—especially in local pickup stations—still heavily rely on manual operations. Staff members are often required to sort, store, and retrieve a vast number of parcels daily, which not only results in high labor costs but also reduces operational efficiency.

From the customer's perspective, picking up parcels at express stations can be inconvenient and time-consuming. Upon arrival, customers must manually search for their package based on shelf codes or barcodes received in a notification, navigating through densely packed and often disorganized shelves. This system becomes even more inefficient during peak periods—such as promotional events or holidays—when express stations experience overcrowding and elevated parcel volumes. As a result, not only does the process become frustrating for users, but it also increases the chances of errors, such as picking up the wrong package. When such mistakes occur, staff must invest additional time and effort to correct them, further straining the system.

To address these issues, we propose an autonomous transport car powered by a robust hardware architecture designed for continuous operation in order to solve these problems. It is able to plan the best routes in real time by automatically scanning and mapping warehouse layouts. With obstacle detection technology, it can safely maneuver around obstacles to deliver packages between storage areas and pickup locations quickly and reliably.

Second, the system features a smart gripping mechanism designed to replace error-prone manual searches. Our robotic arm swiftly recognize and safely grasp packages using sophisticated color recognition technology based on their tagged color labels. This system reduces errors brought on by mismatched barcodes or shelf placements and does away with manual searching.

Lastly, user accessibility and flexible control are given top priority in the solution. Operators have the option of using a streamlined mobile app for everyday tasks or a recognizable PlayStation-style controller for hands-on adjustments during complex scenarios. Staff can quickly resolve exceptions and notify customers of instant pickup thanks to the app's real-time updates on parcel locations and system status. The dual control modes balance speed and accuracy during peak hours by enabling smooth transitions between fully automated and human-guided interventions. When combined, these characteristics reduce the need for labor, speed up service, and improve the experience for end users and warehouse teams.

1.2 Block Diagram

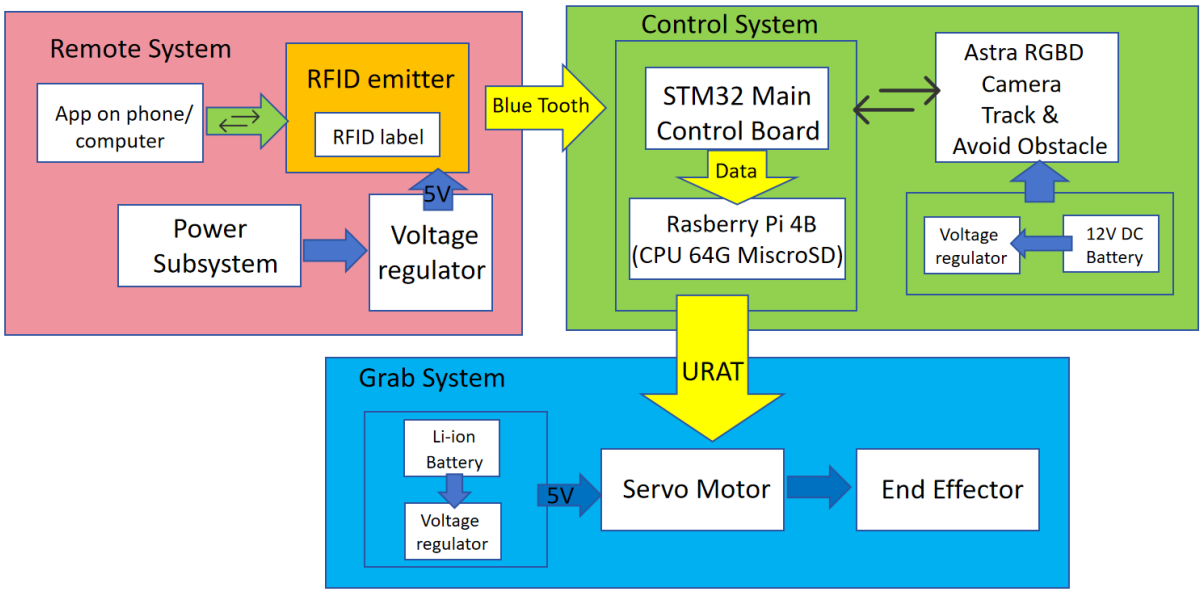

Figure 1: Block Diagram

1.3 Subsystem Overview

1.3.1 Remote System

The remote system consists of two subsystems: PS2 Controller Subsystem and Mobile Application subsystem.

PS2 Controller Subsystem: Designed for precision manual control, the PS2 controller maps its analog joysticks and action buttons to specific vehicle functions. The left joystick governs forward/backward movement and incremental speed adjustments, while the right joystick enables precise steering. Dedicated buttons activate the gripping mechanism: one button adjusts the claw's vertical tilt angle, another controls its horizontal rotation, and a trigger initiates the grasp/release sequence. Tactile feedback ensures operators can fine-tune maneuvers during complex retrieval tasks, such as extracting parcels from tightly packed shelves. The ergonomic design minimizes fatigue during prolonged use, making it ideal for staff training or troubleshooting scenarios requiring direct intervention.

Mobile Application subsystem: The cross-platform mobile app offers both automated and manual control modes. In manual mode, users employ touchscreen directional pads or gesture-based swiping to remotely steer the vehicle, with real-time camera feedback from the car's onboard lens. For automated workflows, the app allows warehouse staff to input destination coordinates or select storage zones on an interactive map, triggering autonomous navigation. Advanced features include priority task queuing (e.g., expediting

urgent deliveries) and system status monitoring, such as battery levels or obstacle alerts. The app's minimalist interface ensures accessibility for users with varying technical proficiency, while encrypted Bluetooth pairing guarantees secure communication.

Operation Process: Upon activation, operators pair either the PS2 controller or mobile app with the car's Bluetooth module through a one-time authentication protocol. During manual control, the PS2 controller's input signals or the app's touch commands are instantly relayed to the vehicle, enabling real-time directional adjustments and claw actuation. For automated tasks, the app converts high-level location targets into navigational paths, which the car executes while continuously sharing positional updates. The system supports dynamic mode switching—for instance, using the PS2 controller to manually reposition the car during app-guided automated retrieval if unexpected obstacles arise. All commands and sensor data are logged for performance analytics, ensuring traceability and enabling continuous optimization of warehouse workflows.

1.3.2 Grab System

The grab system comprises two independent components: the end-effector and servo motors. The robotic arm's mechanical structure features four joints, each connecting rigid arm segments that form an articulated chain configuration.

The first joint serves as the base rotation mechanism, actuated by a servo motor positioned at the arm's bottom. This joint enables 360-degree horizontal rotation of the entire robotic arm. The remaining joints control the movement of individual arm segments within specific planes, each driven by dedicated servo motors. Through coordinated motion of these joints, the robotic arm achieves precise positioning in three-dimensional space.

Mounted at the robotic arm's terminal is the end-effector, designed to execute goods-grabbing tasks. To ensure secure grasping, the end-effector is equipped with rubber bushings that enhance frictional force between the effector and the object. These bushings feature anti-slip textures, allowing adaptation to various item shapes and surface materials.

The servo system employs ZP-series servo motors, capable of achieving high-precision angular control with an accuracy of 0.3 degrees. These motors support dual control methods: serial port (UART) and pulse-width modulation (PWM), enabling precise position and speed regulation via commands from the host controller. This configuration provides stable power transmission for the robotic arm's motion control, ensuring repeatable and accurate movements during operational tasks.

Operation Process:

When the cart arrives at the correct shelf—guided by a black line on the ground—the control system reads data from the RFID reader. This data helps calculate the path that the robotic arm needs to follow. The robotic arm then moves its joints to place the gripper in the right position to pick up the package.

Each joint of the robotic arm uses a high-precision servo motor. These motors let the arm

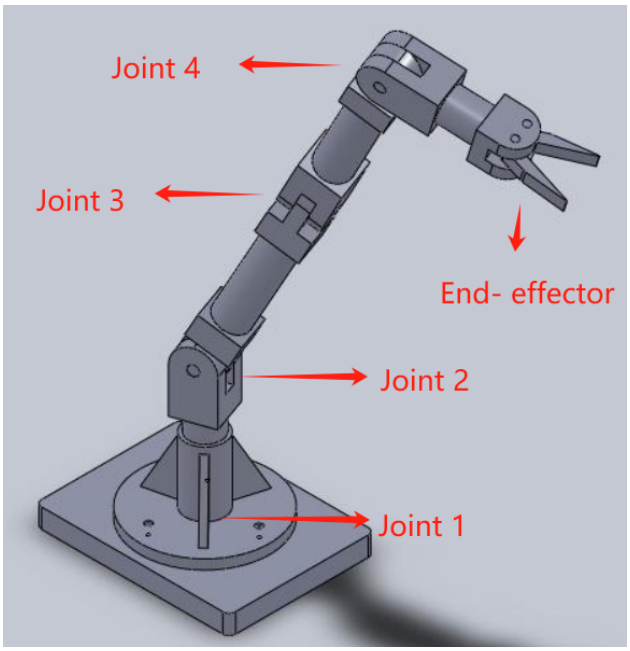

Figure 2: Robotic Arm

parts rotate or move in a straight line, depending on what the task requires. By working together, the joints help the gripper reach the correct spot, no matter how high, deep, or angled the shelf is. The control system uses the RFID location data along with the robotic arm's movement model to control the whole grabbing process. This allows the robot to pick up packages smoothly and accurately, with very little error.

1.3.3 Car System

The car system comprises three independent subsystems: the control subsystem, tracking subsystem, and obstacle avoidance subsystem, each designed for specialized operational roles.

The control subsystem integrates STM32 and Raspberry Pi control boards, serving as the central hub to coordinate the operations of all subsystems. These boards handle data processing, command distribution, and real-time system monitoring, ensuring seamless collaboration between hardware and software components.

The path planning and obstacle detection functionalities are enabled by a depth-sensing camera module. For navigation, the camera actively tracks a pre-marked black guidance line on the ground to maintain the designated route, while its obstacle avoidance capability relies on visual recognition algorithms to detect and identify obstacles—such as stationary objects or other moving carts within the vehicle's proximity.

Operation Process:

After receiving the destination instructions from the main control system, the tracking system uses a preloaded map to plan the best path. The car then follows a black line

on the ground to move accurately along the route. Its built-in camera keeps watching the road ahead to check for any obstacles. If something blocks the way, the obstacle avoidance system will react by slowing down, changing direction, or stopping, to make sure the car moves safely.

When the car arrives at the target location, it waits while the grab system picks up the item. Once the item is confirmed to be picked up successfully, the tracking system calculates the best way to return and guides the car back to the pickup area. Throughout this process, the system constantly uses real-time data from the camera and the control board to support accurate and reliable autonomous navigation.

Figure 3: Car

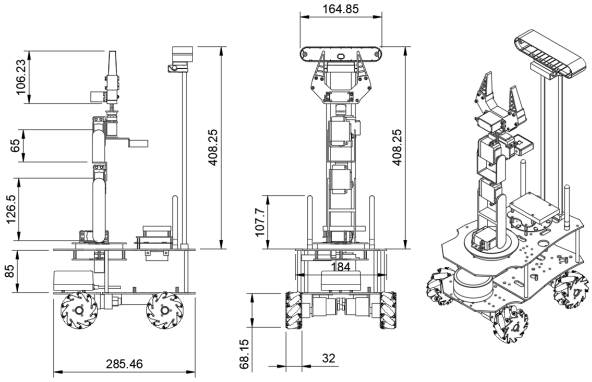

Figure 4: Dimensions of the Car

2 Design

2.1 Subsystem Descriptions

2.1.1 Remote System

PS2 and Mobile Application Subsystem

The PS2 Controller Subsystem was implemented through an STM32 microcontroller acting as the central processing unit, bridging the wireless PS2 controller's inputs to the vehicle's motion and gripper operations. The subsystem leverages the STM32's SPI interface to establish low-level communication with the PS2 receiver module, which decodes radio-frequency signals from the handheld controller. During initialization, the microcontroller configures the SPI peripheral to operate in master mode, synchronizing data transmission with the PS2 receiver's protocol timing. Custom firmware continuously polls the receiver at 100Hz intervals to capture real-time button states and analog stick positions, translating raw hexadecimal data into actionable commands through bitmask operations and scaling algorithms. Each button and joystick axis was programmatically mapped to specific vehicle functions. The left analog stick's vertical displacement governs the vehicle's forward/backward speed through a proportional control algorithm, while the horizontal axis of the right analog stick dictates steering angles via pulse-width modulation (PWM) signals sent to the steering servo. Tactile buttons are assigned discrete actions: the button increments the gripper's rotational position in 5-degree steps, the button triggers a predefined gripping sequence (close, secure, and release), and the L1/R1 shoulder buttons enable fine-grained speed modulation. To prevent unintended inputs during operation, the firmware incorporates debounce logic for digital buttons and a moving average filter for analog signals, ensuring stable command interpretation. The STM32 simultaneously manages a secondary Bluetooth channel for mobile app integration, employing a priority-based arbitration system. When both PS2 and app commands are received, the PS2 inputs take precedence to allow operators to override automated tasks during emergencies. This dual-channel architecture ensures seamless transitions between manual control (via PS2) and semi-autonomous operation (via app), with all command histories logged to internal flash memory for diagnostic purposes. The implementation achieves sub-20ms end-to-end latency from button press to actuator response, validated through oscilloscope measurements of signal propagation across the SPI bus and motor driver outputs.

5V Regulator

We will employ the LMZ12003 3-A Simple Switcher as the core component of our voltage regulator circuit. This SIMPLE SWITCHER® power module provides a user-friendly, step-down DC-DC conversion solution, supporting loads of up to 3 A with high efficiency, excellent line/load regulation, and precise output accuracy. The LMZ12003 features an innovative package design that improves thermal performance and supports both manual and machine soldering. It accepts a wide input voltage range and delivers an adjustable, highly accurate output voltage as low as 0.8 V. The design requires minimal external components—just three resistors and four capacitors—to form a complete

power solution. For reliability, the LMZ12003 integrates multiple protection mechanisms, including thermal shutdown, input undervoltage lockout, output overvoltage protection, short-circuit protection, output current limiting, and prebiased output startup capability. Additionally, the switching frequency (up to 1 MHz) can be set using a single resistor. Our circuit schematic is provided below, with the PCB layout detailed in **Appendix A**.

2.1.2 Grab System

Adapter plate for manipulator

To enable the control board to operate the manipulator, we use servo motors for actuation. The PCA9685 chip serves as the core of the manipulator's adapter board, providing 16-channel PWM signal output for precise servo motor control. As illustrated in Figure 6, PCA9685 regulates servo positioning while receiving a stable voltage supply. Communication with the main control board is facilitated through H1 (PWM signal output) and J1 (data communication). Additionally, to power the servos and other manipulator electronics, an upper adapter plate is implemented, as shown in Figure 7.

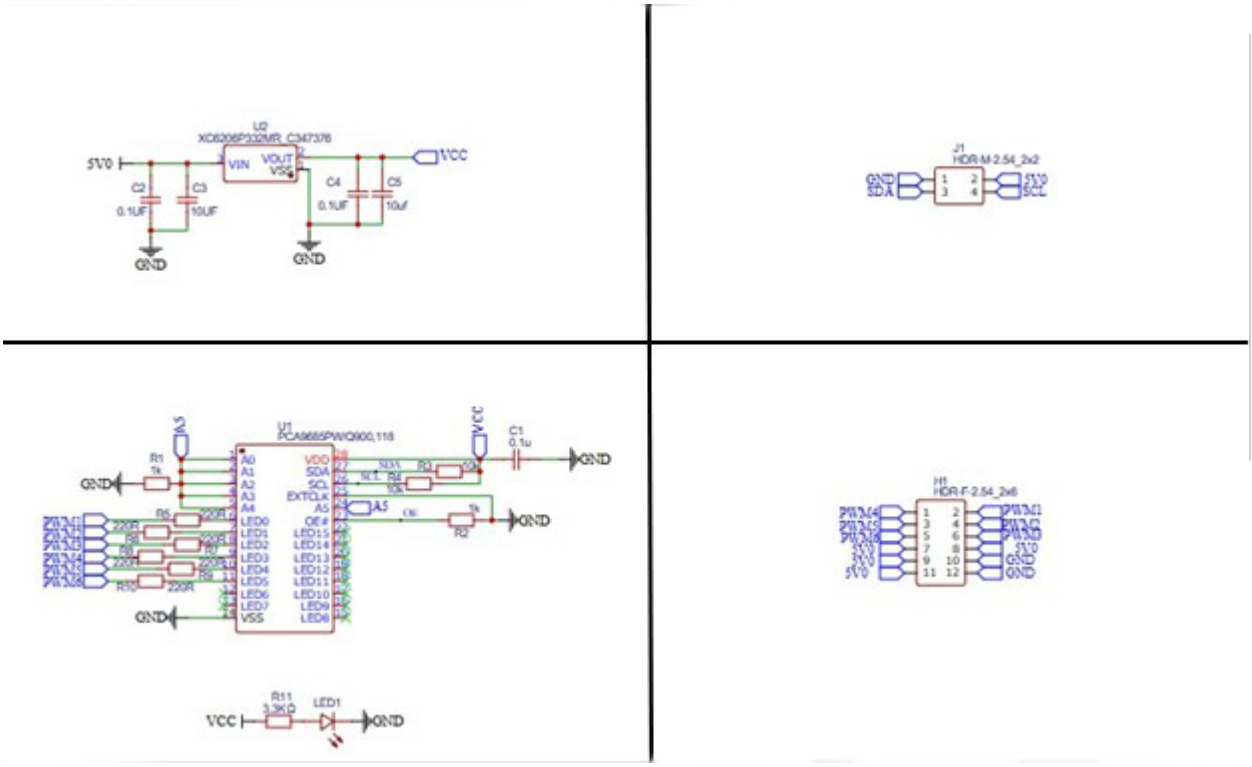

Figure 5: Adapter plate for manipulator (lower plate)

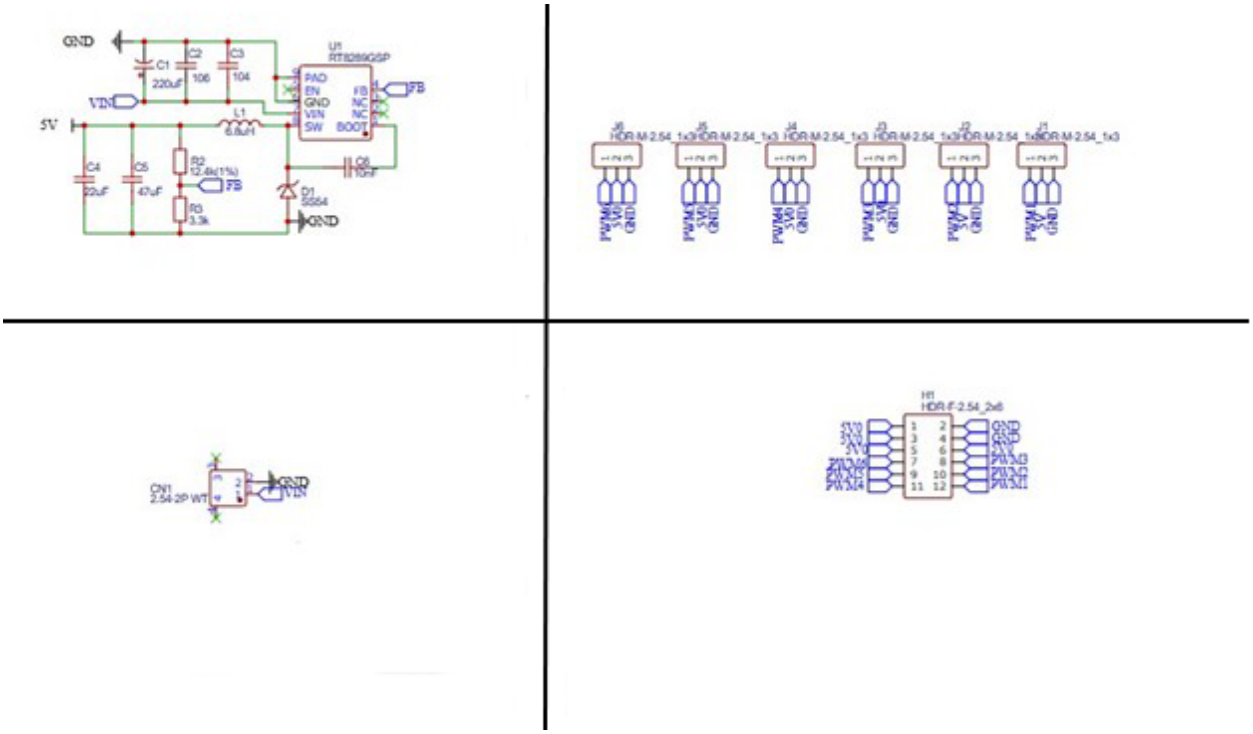

Figure 6: Adapter plate for manipulator (upper plate)

Servos

To realize the working of the robotic arm at all angles, we choose S20F 270° digital servo with 270° operation angles. Parameters of the servo are shown in table 2 and figure 8.

Operating voltage	5V 6.5V
No-load current	80mA (5V)
No-load RPM	0.18 sec/60° (5V), 0.16 sec/60° (6.5V)
Blocking torque	20kg·cm (5V), 23kg·cm (6.5V)
Blocking current	1.8A (5V)
Standby current	4mA (5V)
Reduction ratio	268:1
Physical dimension	40mm×20mm×40mm
Weight	62g
Pulse width range	500 → 2500 sec
Operation angle	270°

Table 1: Parameter of S20F 270° digital servo

2.1.3 Car System

Lithium Battery

The main control panel uses a 12V lithium battery (5600mAh capacity, 0-3A output) with a standard DC 5.5-2.1mm charging port. This battery provides enough power for motors and other parts to work properly. Its performance details are listed in Table 3.

Depth Camera / 3D camera imaging principle

Unlike standard 2D cameras, 3D depth cameras (also called depth-sensing cameras) can measure the distance between objects and the camera. They work by using two lenses separated by 5cm – similar to human eyes – to capture two slightly different images. This difference, known as parallax, occurs because each lens sees the scene from a different angle. After capturing these images, the camera's processor calculates depth information by analyzing the parallax differences, converting the 2D pixel coordinates (x,y) into complete 3D spatial coordinates (x,y,z). These 3D coordinates allow accurate reconstruction of real-world environments for applications like 3D modeling and object distance measurement.

The technology mimics how human vision works: when our brain receives two images from eyes spaced 5cm apart, it automatically detects parallax to judge object positions. As

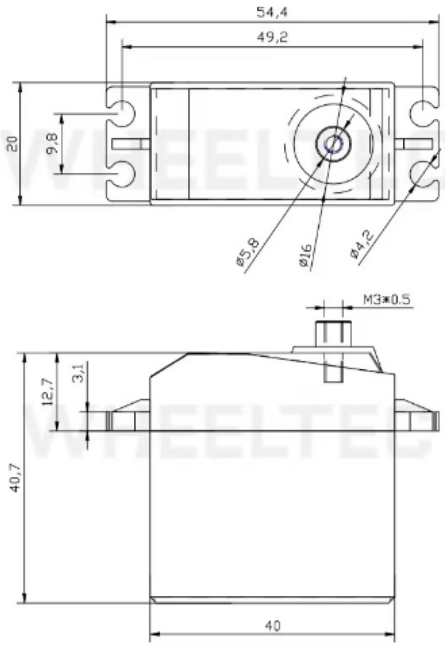

Figure 7: Dimensions of servo

Function	Performance
Voltage supply	+12V DC
Cut-off voltage	9V
Charging current	2A
Fully charged voltage	12.6V
Maximum instantaneous discharge current	13A
Maximum continuous discharge current	6A
Physical dimension	98.5mm×68.5mm×26mm
Weight	268g
Battery protection	Protection for short-circuit, over-current, over-charging and over-discharging, built-in safety valve

Table 2: Performance of the power supply

shown in Figure 9, the camera system replicates this process using polarized lenses and computer algorithms instead of biological vision. Table 4 lists key technical parameters of this depth camera, including its image resolution and depth measurement accuracy.

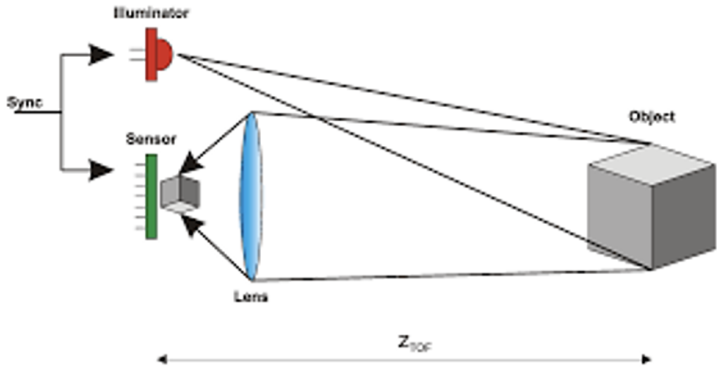

Figure 8: 3D Camera

Depth range (meters)	0.4-2.0
Power consumption	$<$ 2W, peak current $<$ 500mA
Depth map resolution	1280x1024@7FPS 640x480@30FPS 320x240@30FPS 160x120@30FPS
Color map resolution	1280x960@7FPS 640x480@30FPS 320x240@30FPS
Accuracy	1m: ±1-3mm
Depth FOV	H 58.4° V 45.5°
Color FOV	H 63.1° V 49.4°
Delay (ms)	30-45
Data transmission	USB 2.0 or above
Microphone	Two-channel stereo sound
Supported operating system	Android / Linux / Windows7/8/10 / ROS
Power supply method	USB
Working temperature	10°C - 40°C
Size (mm)	165 length × 40 thickness × 30 height

Table 3: ORBBEC camera parameters

Structured light

Previous 1 of 2 Next Human Score: 98.22For an ORBBEC camera, we used structured light technology to implement depth sensing in our self-driving car project. The infrared laser outside the visible spectrum is normally the type of light used for this application. The system calculates both the position and depth of the object as it projects a coded light pattern and captures the returned signal. More specifically, the laser at the designated wavelength is turned on to illuminate the object being analyzed. A CMOS camera that is equipped with a filter for that wavelength captures the light. An onboard ASIC chip processes the picture containing the distorted pattern to obtain depth information from the pattern change.

The core principle involves a triangulation approach, where the laser projection module and the camera are positioned at two distinct spots with a fixed baseline between them. The camera is set at a known distance from a reference calibration plane. When the laser projects its pattern, each point on the object's surface reflects a scattering spot, which is displaced compared to where that spot would appear on the reference plane. By measuring this offset in the x-direction between the distorted pattern on the object and the undistorted pattern on the calibration plane, the system can accurately compute the depth (Z-coordinate) of each point on the object's surface.

The ORBBEC solution we adopted uses diffuse structured light, a variant that utilizes random diffraction spots produced when laser light scatters off a rough surface or penetrates semi-transparent materials like frosted glass. These scattered spots form highly randomized patterns that change with distance, and no two points in space will generate identical scattering distributions. This randomness allows the system to effectively mark the entire 3D space. Once an object enters this marked space, its position can be inferred by observing how the known pattern is altered across its surface. However, this requires an initial calibration of the light field within the environment so that any deviation from the reference can be compared and measured.

The diffuse structured light approach has several advantages. It is a mature and well-established technique that supports a compact hardware design due to the small required baseline between the camera and laser. It is also efficient in terms of computational and power resources, as a single infrared frame is sufficient to compute depth. Since the system uses its own active light source, it functions well even in low-light or nighttime conditions. Moreover, it offers high resolution and accuracy within a limited range, with resolutions up to 1280x1024 and frame rates reaching 60 frames per second.

However, there are also limitations. The system is highly sensitive to ambient light, which makes it less effective in outdoor environments where sunlight can interfere. In addition, the accuracy of depth measurements tends to degrade as the distance from the camera increases, limiting its performance in long-range scenarios.

Path-finding Subsystem

The path-finding system is developed based on the ROS framework. It integrates LiDAR mapping and multi-algorithm path planning capabilities: leveraging LiDAR to col-

lect environmental data, constructing 2D grid maps using the gmapping algorithm (with support for switching to hector/karto algorithms), and saving them as pgm/yaml files via the map_server. Path planning relies on the move_base framework, employing the A* algorithm to generate globally optimal paths and combining DWA/Teb algorithms with costmaps for dynamic obstacle avoidance, expanding safety margins through inflation radii. We utilize tf coordinate transformations and Extended Kalman Filtering (EKF) to fuse visual data, achieving precise localization that supports manual initial pose setting in rviz and loop closure detection for trajectory correction. The trolley's parameters (e.g., maximum speed, acceleration, map resolution) can be dynamically adjusted via rosparam, and it interfaces with the STM32 control subsystem, depth camera obstacle avoidance, and remote APPs. Upon receiving target coordinates, it automatically generates navigation tasks, enabling efficient mapping, precise localization, and dynamic obstacle avoidance in complex environments such as express delivery warehouses.

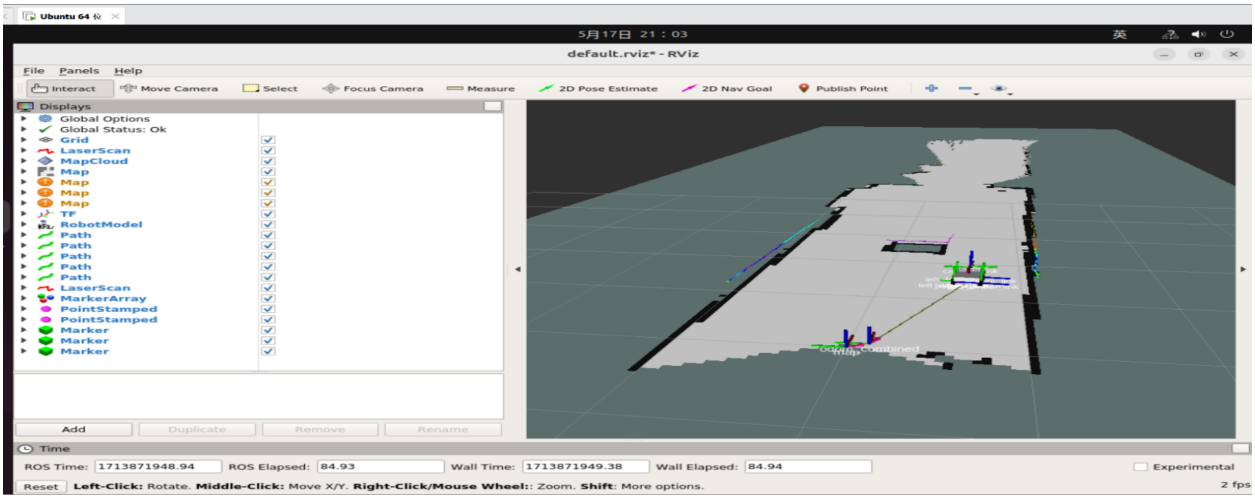

=

Figure 9: Path Finding Interface

STM32F407VET6 Micro-controller

The STM32F407VET6 microcontroller serves as the core processing unit, built around a 32-bit ARM Cortex-M4 processor operating at 168MHz. It includes 1MB of Flash memory for program storage and 192KB of SRAM for temporary data processing. This chip supports advanced features such as a floating-point unit (FPU) for fast mathematical calculations and a memory protection unit (MPU) to enhance system security. Its multiple input/output interfaces include three 12-bit analog-to-digital converters (ADCs) for sensor data collection, two digital-to-analog converters (DACs), and specialized timers for motor control (two 16-bit PWM timers and two 32-bit timers).

The microcontroller connects to external devices through communication protocols like CAN bus for automotive systems, SPI for high-speed data transfer, and USB for peripheral connections. It also integrates a camera interface for direct connection to CMOS sensors and an FSMC (Flexible Static Memory Controller) to manage external memory mod-

ules. Power is supplied through a 12V lithium battery regulated to the required 1.8-3.6V operating range. Figures 11-13 illustrate its connections to motors, Bluetooth modules, and other components, while Table 5 lists its full specifications.

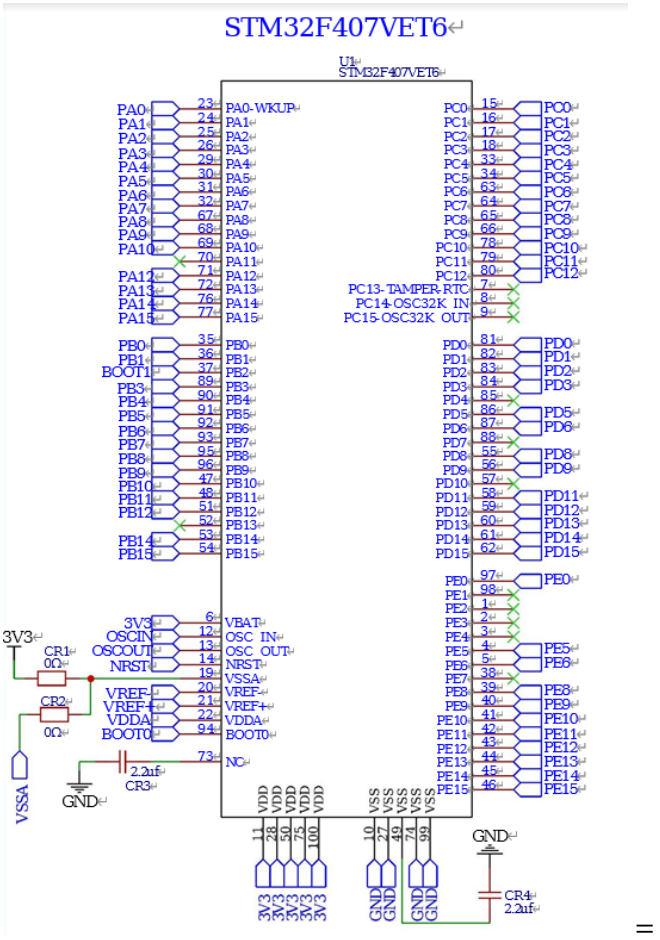

Figure 10: STM32F407VET6 Main Control Board Layout

Motor Driver

The AT8236 motor driver controls the car's DC brush motors, supporting bidirectional rotation and speed adjustment. It operates at voltages from 5.5V to 36V, delivering up to 6A of peak current (4A continuous) for driving high-torque motors. Speed is regulated using PWM (pulse-width modulation) signals from the microcontroller, and its built-in safety features include over-current protection, short-circuit detection, and automatic shutdown during overheating.

The driver uses synchronous rectification technology to reduce energy loss, improving overall efficiency. Packaged in an ESOP8 format with a thermal pad, it efficiently dissipates heat even during heavy use. Figure 14 provides the pin layout, showing connections for power input, motor outputs, and control signals. This lead-free design meets environmental safety standards and is suitable for automotive applications.

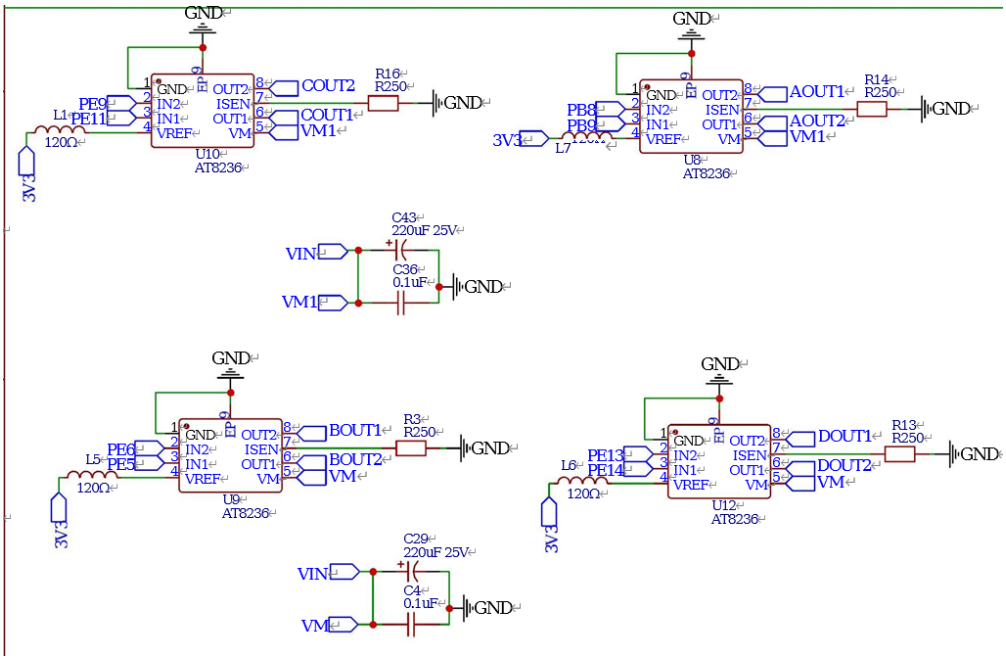

Figure 11: Motor drive circuit

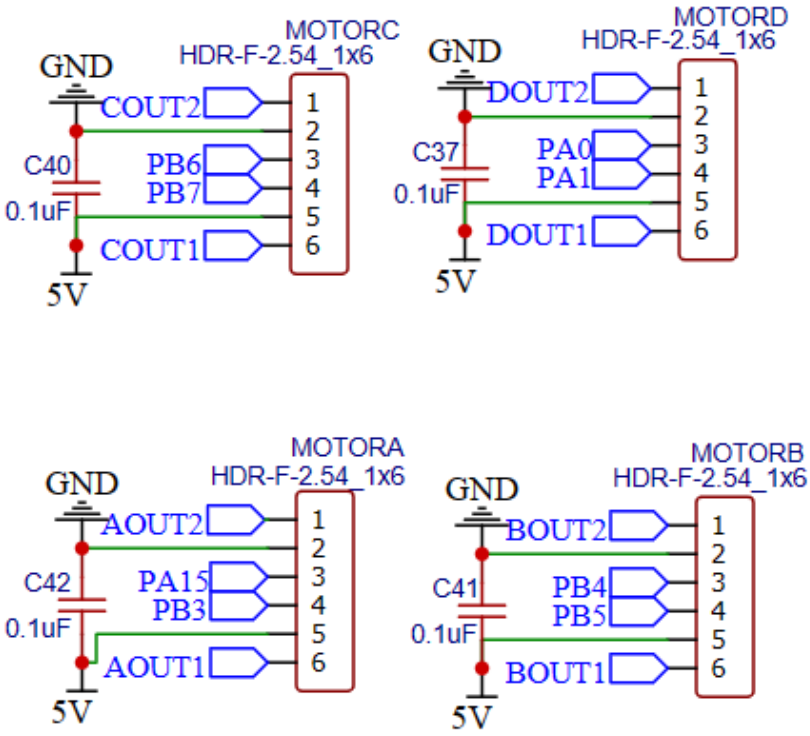

Figure 12: Motor Encoder Interface

I/O Number	Connection	Function
PA12	LED	Power indicator
PD11, PD12, PD13, PD14	OLED	Display the working status of the car
PD5, PD6	Bluetooth	For the wireless communication with users through app on their phones
PB8, PB9	Motor A	Control the McNamee wheel of car
PE5, PE6	Motor B	Control the McNamee wheel of car
PE9, PE11	Motor C	Control the McNamee wheel of car
PE13, PE14	Motor D	Control the McNamee wheel of car
PA15, PB3	Motor A encoder	Locate the exact position of the car
PB4, PB5	Motor B encoder	Locate the exact position of the car
PB6, PB7	Motor C encoder	Locate the exact position of the car
PA0, PA1	Motor D encoder	Locate the exact position of the car
PC6, PC7, PC8, PC9, PB14, PB15	Model/Servo Interface	For the remote control
PD3	Motor enable switch	Switch to control the motor

Table 4: STM32F407VET6 Main Control Board Resource Allocation

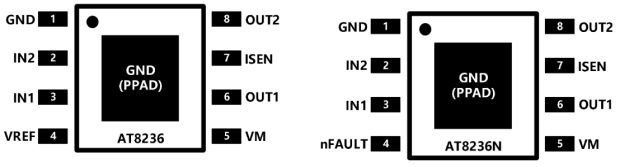

Figure 13: AT8236

Raspberry Pi 4 Model B

The Raspberry Pi 4 Model B acts as the secondary computing unit, handling complex tasks like sensor data analysis and wireless communication. It features a 64-bit quad-core Broadcom BCM2711 processor running at 1.5GHz, paired with 4GB of LPDDR4 RAM for multitasking. Video output is supported through dual micro-HDMI ports capable of 4K resolution, while a dedicated hardware decoder enables smooth 4K video playback.

Network connectivity includes dual-band Wi-Fi (2.4GHz/5GHz), Bluetooth 5.0 for device pairing, and a Gigabit Ethernet port for wired connections. Four USB 3.0 ports allow high-speed data transfer with external devices like cameras or storage drives. The system boots from a microSD card running a Linux-based OS and interfaces with the STM32 microcontroller via UART and GPIO pins for coordinated control. Its modular certification simplifies integration into final products, reducing development time and compliance costs.

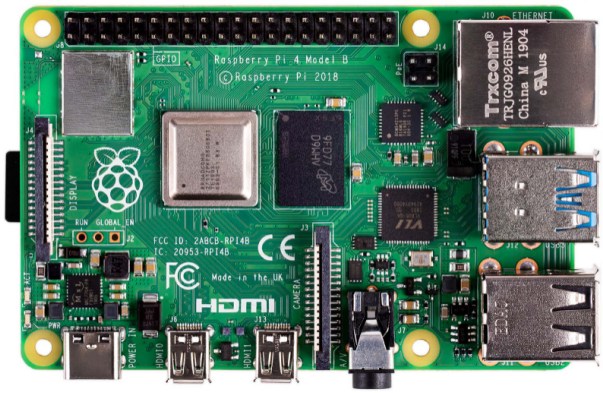

Figure 14: Raspberry Pi 4 Model B

2.2 Subsystem Verifications

2.2.1 Remote System

Requirements and Verification Table of Remote system

Requirements	Verification
The mobile phone uses Bluetooth to communicate with the car module.	1. Verify that the mobile phone correctly receives the trolley's transmitted data. Measure and log the communication delay. Conduct repeated tests to confirm communication stability, ensuring a success rate of larger than 95% at the maximum operational distance within the designated environment. 2. Gradually increase the separation distance between the trolley and mobile phone until stable communication fails. Record the maximum reliable communication distance, which must exceed 1.5 times of the farthest operational distance required in the application scenario.
Express pickup range is large	1. Given that RFID has a limited recognition range of 0-4m, we employ a grouping method for short-distance item identification. 2. Like the approach used in courier stations, we assign identification numbers to shelves and utilize depth camera visual recognition to initially locate the target shelves. 3. Upon reaching the designated shelves, we activate the RFID reader module to pinpoint the exact location of specific goods.
5V Regulator PCB Board	1. A well-manufactured PCB board is connected to an independent 12V lithium battery, with an oscilloscope monitoring the output voltage to ensure it remains within the 4.5V-5.5V range while maintaining stable waveform characteristics. 2. When connected to the RFID read-write module, the module should demonstrate normal functionality, requiring thorough testing to verify proper read-write operations.

2.2.2 Grab System

Requirements and Verification Table of Grab system

Requirements	Verification
Every segment of the manipulator can rea -ch up to 270° without any load and under a 12V power supply	1. Record the initial position of the segment. 2. Connect the servo of the segment to the +12V power supply. 3. Record the final position of the segment until the segment can not move in a certain place. 4. Measure the angle between the initial and final position of the segment.
Grap objects ranging from 2 to 10 cm in dia -meter with the weight ranging from 200g to 300g.	1. Prepare a set of objects ranging from 2 to 10 cm in diameter with varying surfaces and varying weight from 200g to 300g. 2. Program the robotic arm to attempt to grasp each object using its standard operating procedure. 3. Record whether each grasp is successful (object is securely held) and note any damage to the objects.

2.2.3 Car System

Requirements and Verification Table of Car system

Requirements	Verification
The car system must sustain rated speed under payload conditions.	1. Test if the car can well drive and turn at speed greater than 0.3m/s in case of no grasping. 2. Test sustained operation at rated speed while carrying maximum approved load capacity. 3. Use a multimeter to measure the operation of the motor, ensure there is no idling or other conditions that can lead to motor burnout.
The depth camera must maintain stable imaging quality during vehicle operation.	1. Ensure the depth camera maintains stable imaging through secure mounting and vibration reduction measures. 2. Keep the car run at the rated speed and use the visual recognition algorithm to evaluate and ensure that the recognition accuracy reaches more than 95%.
The can cannot turn over in the process of grasping objects while driving	1. Keep increasing the weight of the goods, test the grasping process of the car until the car appears to be tipped over, record the grasping limit of the car. 2. Increase the counterweight of the car until the travelling pressure of the car and the weight of the gripped goods are well balanced.

2.3 Design Alternatives

2.3.1 Past Version

Figure 15: Past Version of Gripper

As shown in the illustration, this was our initial design for the robotic grabbing hand, which employed multiple elastically rotatable components connected in sequence to simulate human finger grasping motions. However, during practical testing we identified several significant flaws in this design. The primary issue was that the gripper failed to provide sufficient grasping force on the target blocks due to excessive flexible components and weak connection strength. During rapid movement while holding objects, the blocks would frequently dislodge and fall. Additionally, the deformable design of the gripper proved incapable of smoothly adapting its shape to match the contours of different objects. The overall performance of this design proved unsatisfactory, leading us to conclude that substantial modifications and improvements were necessary. We have therefore decided to redesign the grabbing mechanism to address these critical shortcomings.

2.3.2 Improved Version

We have implemented structural improvements to the grabbing hand as shown in the diagram. The new design features multiple elastic components with built-in springs mounted on a rigid base, achieving both automatic shape adaptation and cushioned grasping through elastic buffering. During practical testing, this optimized design demonstrated outstanding gripping performance. It provides sufficient grasping force to securely hold objects even during rapid movement and vibration, with no instances of dropped blocks. The overall structural strength has been significantly enhanced, resulting in more reliable operation. Additionally, the simplified architecture with reduced component count has improved durability while making the mechanism less prone to damage.

Figure 16: Improved Version of Gripper

2.4 Tolerance Analysis

2.4.1 Endurance Calculation

We will use a lithium battery to support the operation of the car and the grabbing system and here we need to calculate the designed maximum working capacity for the car, so the system can satisfy our design requirements. Here we calculate the working capacity of the car at maximum load and output to get the limitation of endurance:

Battery Capacity, $C = 5600\,\text{mAh}$ (only 80% will be used)
Working Current, $I = 3\,\text{A}$, **Working Voltage,** $V = 5\,\text{V}$
Total Working Power, $P = UI = 15\,\text{W}$

For each working course, we assume the car will move 10 [m] on average for each complete delivery, 5 [m] to fetch the goal object and 5 [m] to take to target location, and the designed average moving speed is $0.3\,\text{m/s}$.

In the calculation, we will ignore the RFID tolerance because RFID can last 30 days and won't be a bottleneck, and ignore the effect of the weight of goods on the working power because they're small. When the car is standby and fetching goods, the power cost is low and can be neglected.

As a result, the calculated time the car can work after fully charged:

$$\frac{5600\,\text{mAh} \times 80\% \times 5\,\text{V}}{15\,\text{W}} \approx 5400\,\text{s} = 90\,\text{min}$$

And the total number of times the car can transport the goods is:

$$\frac{5400\,\text{s} \times 0.3\,\text{m/s}}{10\,\text{m}} = 162\,\text{times}$$

In conclusion, these equipments can meet our design requirements for the endurance of the transport car.

2.4.2 Grab Simulation and Test

When evaluating the operation efficiency and security of the grabbing system, the key factor is the risk of turn off when the car is under the load from goods and the holding geometry shape of the arm will change the position of general gravity center. Therefore, the turn off risks mainly come from the dynamic interaction between goods and grabbing arm when fetching and transporting the goods. To verify the security and security, we decide to use methods combining theoretical analysis, simulation and practical tests on the performance of the general system when working in different conditions. The focus point of this part is that the mechanical arm need real-time gravity center adjustment function to improve the stability against turning off. The core mechanism is the grabbing arm will adjust its configuration through algorithm control and motor motivation. The goal is to maintain the gravity center within the range of supporting surface of the bottom trolley and the risk of turning off can be reduced to the least. Through double check from real test and simulation, we have sufficient confidence that the system have well performance in keeping balance from turning off. In conclusion, data analysis from both modeling and testing phases confirms that the robotic arm's control algorithm, with its specialized load-distribution optimization, reduces vehicle rollover probability during cargo handling to negligible levels. This finding demonstrates the inherent safety design considerations embedded in the algorithm's architecture, ensuring operational reliability and safety in real-world applications.

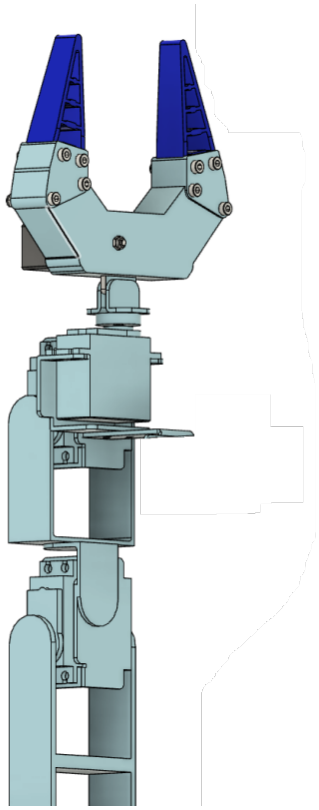

Figure 17: Grab Arm

2.4.3 Velocity and Load Analysis

In this part, we will calculate the weight range of the goods that could be transported by our car and check the strength limitation of the grabbing segments in these cases.

For our car, we use four motors with torque output τ of $4.5\,\text{kg}\cdot\text{cm}$ and power supply P of $4\,\text{W}$ to drive each wheel at designed speed. With the relationship between torque output, angular velocity, and power output:

$$P = \tau\omega$$

where ω is the angular velocity of the motor.

Thus, the minimal angular velocity is:

$$\omega = 9.061\,\text{rad/s}$$

When the motor is without extra load and given the radius of the wheel is $0.038\,\text{m}$, the velocity at the outline of the wheels is:

$$v = 0.344\,\text{m/s}$$

Given the total weight of our car, M, is $4.5\,\text{kg}$ and the friction factor, μ, of the ground is ranging from 0.4 to 0.6, and based on the relationship between the power and force:

$$P = Fv$$

For totally 4 wheels:

$$F = Mg \cdot \frac{\mu}{4}$$

$$4.4145\,\text{N} \leq F \leq 6.62175\,\text{N}$$

So, the velocity at each wheel:

$$0.604\,\text{m/s} \leq v \leq 0.906\,\text{m/s}$$

In our design requirements, we set the minimum speed of the car is at $0.3\,\text{m/s}$, so considering the weight of electronic components and goods, their weight, M_{load},

$$M_{\text{total}} = M + M_{\text{load}}$$

M_{load} should be:

$$M_{\text{load}} \leq 4.56\,\text{kg}$$

Then, eliminating the weight of electronic components at most for 3kg, we apply the rest weight load from goods to the grabbing module segments and do FEA simulation, here are result:

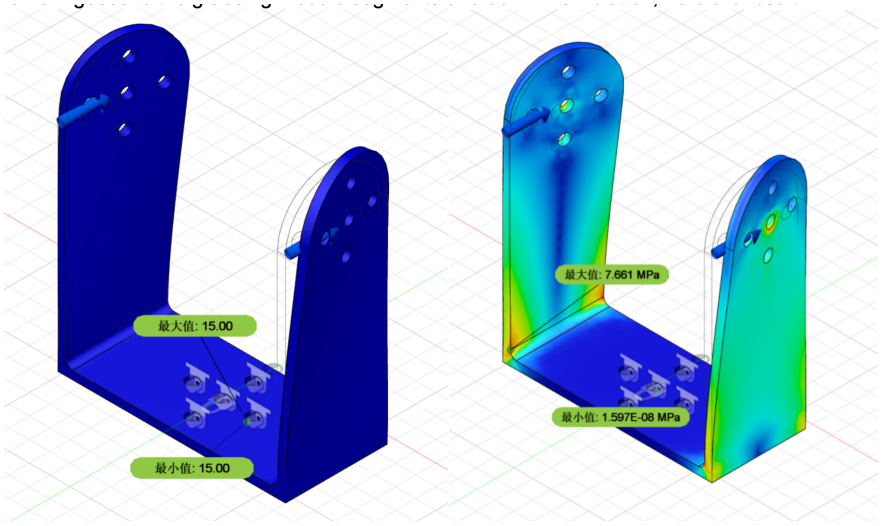

Figure 18: FEA result of the segment

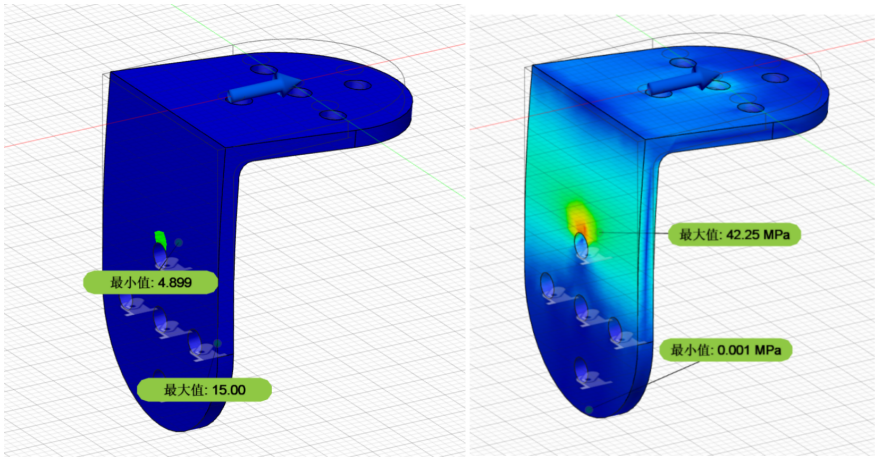

Figure 19: FEA result of the segment

From the FEA simulation, we can get all the safety factors are at least 4.5, ensuring high security and stability for our design against strength failure of the grabbing mechanisms.

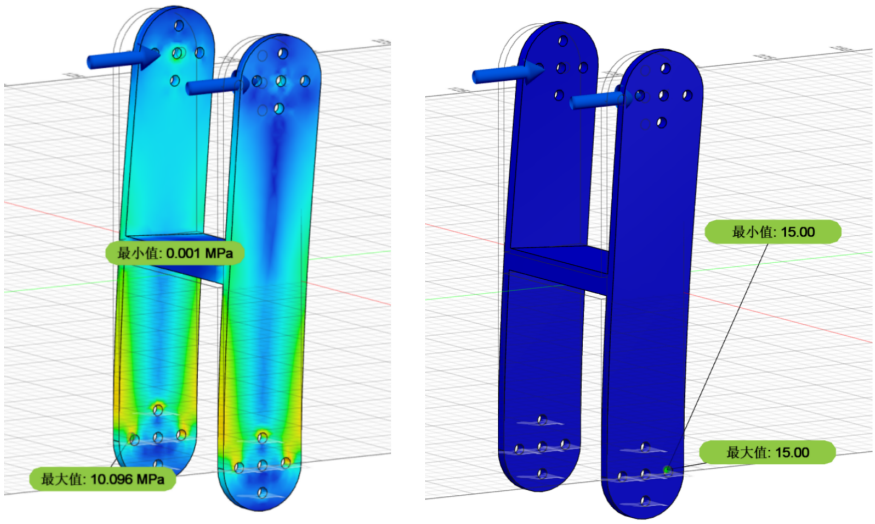

Figure 20: FEA result of the segment

3 Cost & Schedule

3.1 Cost

Here we will do cost analysis. It will include a cost analysis of the project by following the outline below and a list of any non-standard parts, lab equipment, shop services, etc., which will be needed with an estimated cost for each.

- Labor: (For each partner in the project)
- Assume a reasonable salary ($/hour) x 2.5 x hours to complete = TOTAL

  Then total labor for all partners. It's a good idea to do some research into what a graduate from ECE at Illinois might typically make.
- Parts: Include a table listing all parts (description, manufacturer, part , quantity and cost) and quoted machine shop labor hours that will be needed to complete the project.
- Sum of costs into a grand total

3.1.1 Labor

According to the table 6 The following are the labor costs calculated based on the actual workload of our projects and the course hours required after taking into account the hourly rates of senior design projects and UIUC internships in previous years.

Partner	Hourly Salary	Working Hours	Total
Yiqi Tao	$35	200	$35 * 200 * 2.5 = $17500
Xubin Shen	$35	200	$35 * 200 * 2.5 = $17500
Jingyuan Ma	$35	200	$35 * 200 * 2.5 = $17500
Haotian Zhang	$35	200	$35 * 200 * 2.5 = $17500
Sum			$70000

Table 5: Labor Cost

3.1.2 Parts

The estimated parts cost is listed in Parts Cost Analysis table. The estimated cost is about $650.

Description	Manufacturer	Vendor	Quantity	Cost/Unit	Total Cost
12V 0-3A 5600mAh Lithium Battery	Wheeltec	Taobao	3	17.53	52.59
5V Regulator	Self Design PCB	J@LC	2	10	20
RFID Read and Write Module	FK	Taobao	1	53.27	53.27
RFID Labels	FK	Taobao	20	0.087	1.74
STM32F407VET6 Main Control Board	Wheeltec	Taobao	1	63.7	63.7
Raspberry Pi 4B(CPU GPU/NPU 64G MicroSD)	Wheeltec	Taobao	1	129.67	129.67
Astra RGBD Camera	Wheeltec	Taobao	1	138.1	138.1
6 joint robotics arms	Wheeltec	Taobao	1	98.3	98.3
Car Board	Wheeltec	Taobao	1	26.8	26.8
MG513 Motors	Wheeltec	Taobao	4	11.2	44.8
Shelves	JD	JD	2	7.78	15.56
Loads	JD	JD	20	0.035	0.7
Total					644.33

Table 6: Parts Cost Analysis

3.1.3 Total Cost

The Total cost of labor and parts is $\$70000 + \$644.33 = \$70644.33$

3.2 Schedule

The weekly schedule is listed in the table 8 below.

Week	Yiqi Tao	Xubin Shen	Jingyuan Ma	Haotian Zhang
3/23-3/29	Check components ports	Combine car and robotic arm	Check the power system	Check the robotic arm
3/30-4/5	PCB Board Design and Test	Robotic arm coding	RFID coding	Tracking coding
4/6-4/12	Test Power Subsystem (regulator)	Test the robotic arm moving and grabbing	RFID test	Test the camera
4/13-4/19	Test the system of tracking with camera	Test the grab subsystem in the environment	App coding	Finish the robotic arm control while grabbing
4/20-4/26	Test subsystem and debug	Test subsystem and Debug	Test subsystem and Debug	Test subsystem and Debug
4/27-5/3	Integrate, finalize decoration	Integrate all	Integrate all	Integrate all
5/4-5/10	Mock Demo	Mock Demo	Mock Demo	Mock Demo
5/11-5/17	Prepare for Final	Prepare for Demo	Prepare for Demo	Prepare for Demo
5/18-5/24	Individual Report	Individual Report	Individual Report	Individual Report

Table 7: Weekly Schedule

4 Conclusion

4.1 Project Outcomes

In this project, we innovatively designed and implemented an unmanned transport vehicle with the function of autonomous color recognition. This device consists of a remotely controlled trolley and a mechanical grasping arm. It can intelligently map the surrounding environment through an advanced lidar system, automatically plan the traveling route based on the received instructions, and identify the color of the goods for grasping. Complete the designated transportation tasks.

Specifically, the control system of the main body of the car is realized based on Raspberry PI control board and STM32 chip technology. The mechanical grasping and some structural support components are made by 3D printing technology. Different system modules cooperate well, the hardware structure is stable and reliable, and it has a good operational performance. The car is equipped with multiple remote control methods. It can be simply and directly controlled through a remote control or a mobile phone app, or more complex tasks can be input and planned through a dedicated program on a personal computer. The car itself is equipped with a complete algorithm system. Users can complete a series of action tasks by inputting simple instructions.

In actual use, we first control it through a remote program, using the lidar of the trolley to automatically scan and construct the surrounding environment. Then, we input the starting and end points of the transportation task. The trolley program can complete the automatic route planning, avoid possible obstacles on the path, reach the goods, and lock the target goods through the color recognition program for automatic grasping. Then, follow the planned route to reach the designated place and complete the entire transportation task. We are satisfied with the overall operation test results.

4.2 Uncertainties

Although our car performs well overall, there are still some uncertainties in the system that may affect the final performance:

Firstly, the liDAR scanning mapping system of our car requires the car to traverse the entire site to complete a relatively detailed and complete mapping. For some blind spots and deviations during the mapping process, it may affect the accuracy and reliability of the final route planning and navigation. The color recognition of the grasping system requires that the color of the target object has sufficient contrast and discrimination with the surrounding environment, and is easily affected by the environmental lighting conditions. In practical applications, it may have poor adaptability. The connection between the car and the control device relies on the wifi signal. When the signal fluctuates, the communication between the devices deteriorates, and there may be significant delays in commands and responses, affecting stability.

4.3 Future Improvement Directions

The transport vehicle we have designed is based on the transportation work of the vertex given items. It has high requirements for the shape, appearance and color of the objects, as well as the transportation route. It has poor adaptability to the complex and diverse environment and demands in reality. Regarding this, we believe that future improvements can be: Increase the degree of freedom and deformability of the grasping structure to adapt to various grasping requirements, improve the reliability and adaptability of the color recognition function, incorporate features such as the shape of the items into the recognition reference to enhance the accuracy of the recognition system, establish a more efficient path planning management system and the automatic optimization function of the path, and continuously optimize the control and selection of the path in multiple tasks. Improve the overall transportation efficiency and adaptability to the larger environment.

4.4 Ethics

4.4.1 Problems during the development of our project

1. To ensure the reliability and safety of our project, we must carefully select the car motor based on its rated working power and speed to avoid potential issues such as overpowering or burnout. An inappropriate motor choice could lead to premature failure, so it's critical to analyze the system requirements and operating conditions before finalizing the purchase.
2. During the test, short circuit sometimes happened when connecting the driving circuit or the recognizing circuit, so we should design short-circuit protection circuits and regularly check and document progress.
3. Robotic arms should be designed and programmed to prioritize the safety of humans and other living beings in their vicinity. This includes implementing safeguards to prevent accidents, such as collision detection sensors, emergency stop buttons, and fail-safe mechanisms.
4. If the ideal results of the experiments are hard to get, we should make sure that there's no plagiarism or fake and made up figures of the results, according to the IEEE code of ethics, "to seek, accept, and offer honest criticism of technical work, to acknowledge and correct errors, to be honest and realistic in stating claims or estimates based on available data, and to credit properly the contributions of others."[1]

4.4.2 Problems from the accidental or intentional misuse of my project

1. Our transport car is designed in small test size, so if the car is upgraded to a bigger size, risks may happen. For example, when in the factory to fetch come large cargo, the car may run into people and cause injury. That is not considered in our current design.So safety fence can be erected around the shelf and the machine's path for movement.

2. When the machine malfunctions, people who are using it should give feedback in a timely manner and seek repairs.
3. People who operates the machine should be trained according to the IEEE code of ethics, "to maintain and improve our technical competence and to undertake technological tasks for others only if qualified by training or experience, or after full disclosure of pertinent limitations."[1]

References

[1] IEEE. ""IEEE Code of Ethics"." (2016), [Online]. Available: https://www.ieee.org/about/corporate/governance/p7-8.html (visited on 02/08/2020).

Appendix A PCB Design

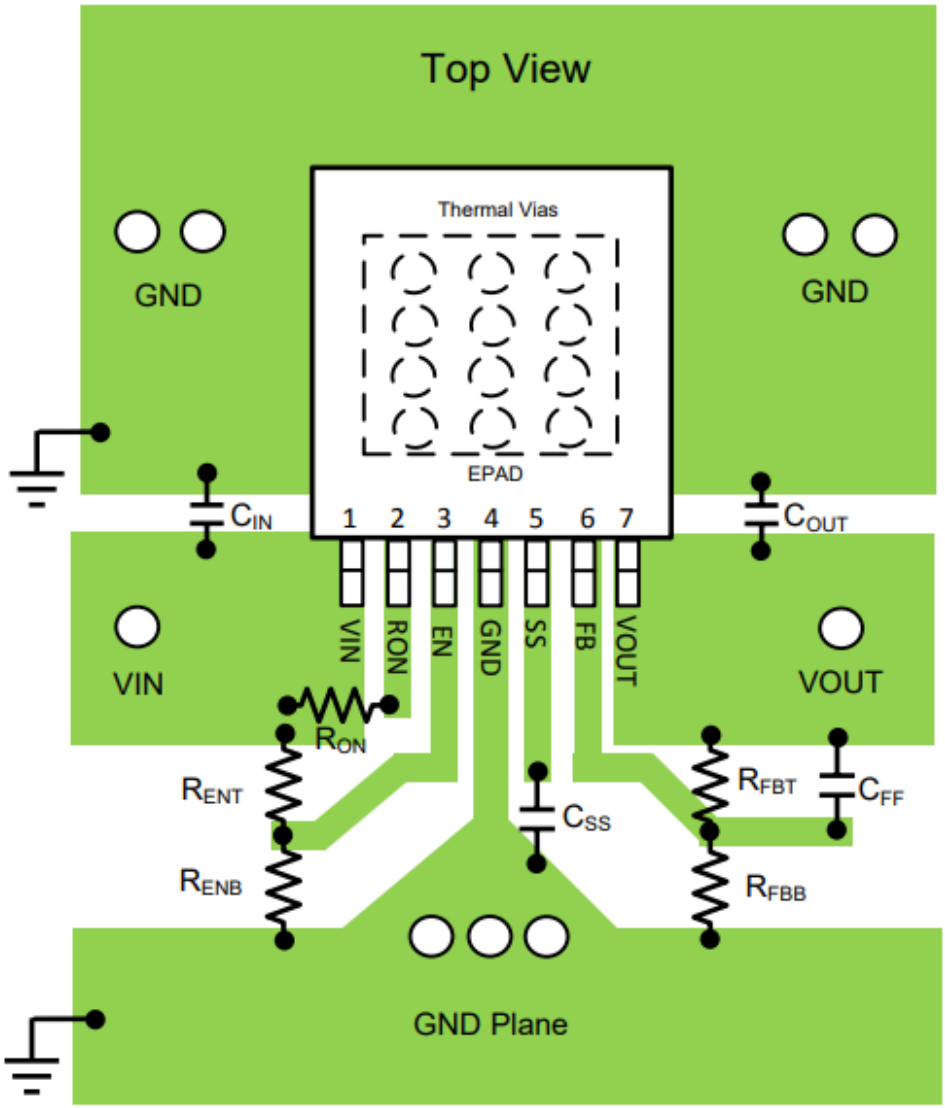

Figure 21: PCB Design